Testing the reversible insertion of magnesium in cationic-deficient manganese oxy-spinel through a concentration cell

Alejandro Medina, Ana I. Rodríguez, Carlos Pérez-Vicente and Ricardo Alcántara

Departamento de Química Inorgánica e Ingeniería Química, Instituto Universitario de Investigación en Química Fina y Nanoquímica (IUNAN), Universidad de Córdoba, Campus de Rabanales, Edificio Marie Curie, E-14071 Córdoba, Spain.

Structure calculation

For the theoretical calculations, the next six structures were employed.

1. ***(1) $MgMn_2O_4$ structure.*** It has a tetragonal spinel structure, s.g. $I4_1/amd$. The tetragonal distortion of the cubic spinel structure is due to the cooperative Jahn-Teller distortion of Mn^{3+} coordination octahedra.
2. ***(2) Mn_2O_4 structure.*** It has a cubic spinel structure, s.g. $Fd\bar{3}m$, with all tetrahedral sites empty.
3. ***(3) $Mg_{0.5}Mn_2O_4$ structure.*** In a spinel structure, the tetrahedral sites occupied can be described as two interpenetrated diamond sub-lattices, as shown in Fig. S1-A. The first neighbors of atoms in the first sub-lattice are just the atoms in the second sub-lattice, and *vice-versa*. When the tetrahedral sites are fully occupied both sub-lattices are also occupied (Fig. S1-B). But when these sites are half occupied, and in order to minimize repulsions between atoms in tetrahedral sites, only one of the sub-lattices should be filled, being the other sub-lattice empty. An alternative description of the same filling is to occupy only half of each tunnel (Fig. S1-C).
4. ***(4) $Mg_{0.75}Mn_2O_4$ structure.*** One of the sub-lattices is fully occupied, and the other lattice is half-occupied.
5. ***(5) $Mg_{0.25}Mn_2O_4$ structure.*** One of the sub-lattices is empty, and the other lattice is half-occupied.
6. ***(6) $Mg_2Mn_2O_4$ structure.*** The Mn_2O_4 cubic spinel framework is retained, and all Mg atoms are located in the empty octahedral sites, to give an "ordered" NaCl-type structure.

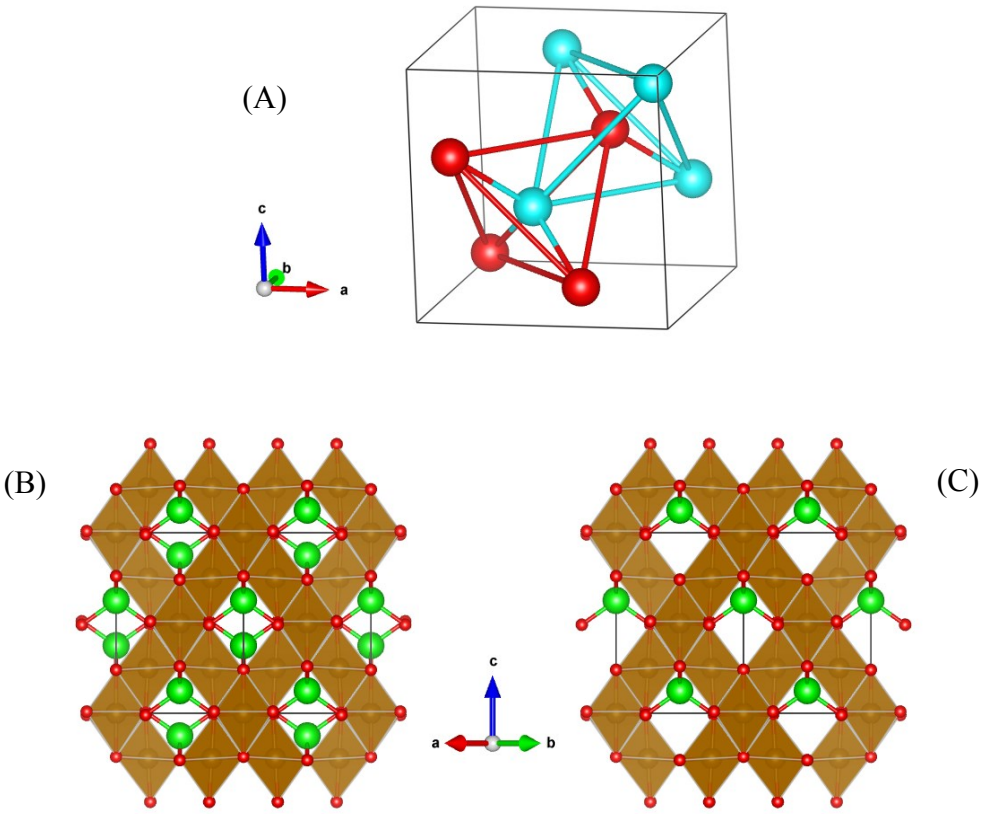

Figure S1. Schema of the tetrahedral sites occupied in a spinel structure: (A) showing the two interpenetrated diamond sub-lattices, (B) 100 % occupation of tunnels (typically 8a site), (C) 50 % occupation of tunnels.

For the calculations, we started using a tetragonal unit cell, as expected for $MgMn_2O_4$, and then Mg atoms were removed, as described above. In all cases, all the parameters were allowed to vary (s.g. P1). The difference between the unit cell parameters "a" and "b" was smaller than $3 \cdot 10^{-4}$ Å. Concerning the unit cell parameter "c", it can be used to evaluate the tetragonal distortion of the structure. For a cubic spinel c/a = 1. As the ratio c/a increases, the tetragonal distortion also increases. For $MgMn_2O_4$ c/a = 1.16 (Table S1), clearly showing the tetragonal distortion, due to cooperative Jahn-Teller distortion due to Mn^{3+} cations. As Mg is extracted, Mn^{3+} is progressively oxidized to Mn^{4+}. As the Mn^{3+} amount decreases, also the tetragonal distortion decreases, evidenced by a progressive decrease of c/a down to ca. 1 for x = 0.25.

Table S1. Calculated cell parameters for $Mg_xMn_2O_4$ ($0 \leq x \leq 1$).

	a, Å	b, Å	c, Å	c/a	Vol./f.u. / Å^3
$MgMn_2O_4$	8.125	8.125	9.426	1.16	77.77
$Mg_{0.75}Mn_2O_4$	8.194	8.194	9.105	1.11	76.15
$Mg_{0.5}Mn_2O_4$	8.215	8.215	8.686	1.06	73.28
$Mg_{0.25}Mn_2O_4$	8.312	8.312	8.251	0.99	71.28
Mn_2O_4	8.150	8.150	8.165	1.00	67.80

Voltage calculation

The voltage of a reaction can be obtained from its free energy according to:

$$\Delta G = -n F \Delta V$$

where ΔG is the free energy of the reaction, n is the number of electrons transferred in the reaction, F is the Faraday's constant and ΔV is the voltage of the reaction. For the magnesium extraction reaction:

$$Mg_xMn_2O_4 \rightleftharpoons Mg_yMn_2O_4 + (x-y)Mg, \qquad where\ x > y$$

The free energy of the reaction is then:

$$\Delta G_R = \Delta G\left(Mg_yMn_2O_4\right) + (x-y)\Delta G(Mg) - \Delta G\left(Mg_xMn_2O_4\right)$$

Thus, the energy of the different phases calculated by DFT method can be used to estimate the voltage of the Mg extraction (insertion) reaction, according to:

$$\Delta V = -\frac{E\left(Mg_yMn_2O_4\right) + (x-y)E(Mg) - E\left(Mg_xMn_2O_4\right)}{2(x-y)\,F}$$

Calculation of percolation energy

The Bond Valence Model (BVM) is based on Pauling's principles of bond order. BVM relates the bond order of chemical bonds to their lengths. As empirical method, BVM is frequently described as a simplistic approach to bonding. Recently, the basis of BVM and its validity were confirmed [E. Levi, D. Aurbach, C. Gatti, Do the basic crystal chemistry principles agree with a plethora of recent quantum chemistry data? IUCrJ, 2018, 5, 542] [E. Levi, D. Aurbacha, C. Gatti, Revisit of the Bond Valence Model makes it universal. Phys. Chem. Chem. Phys., 2020, 22, 13839].

The empirical correlation between the valence and length of a bond allows to estimate the valence if the bond length is known. The sum of all the bond valence (BV) around a given atom should equals its oxidation state. The sites in the structure where the BV sum of a given atom matches its oxidation state can be identify as a possible equilibrium sites for that atom. Locating a cation systematically through the unit cell can generate a valence map in which a point having a value close to the oxidation state of the cation represents a possible location for that cation. Other application is the mapping of diffusion paths between two possible locations for ionic conductors, which should take place trough volume paths where the difference between formal and calculated oxidation states (ΔV) is as smaller as possible. The percolation point between two sites can be obtained by increasing ΔV until a path connecting two sites is found.

The cation/anion interactions can be modeled by using a Morse-type interaction potential, also Coulombic repulsion term should be added (for example, for migration, the repulsion between migrating cation and framework cations). Combining BVM and energy calculations, a Bond Valence Energy Landscape can be obtained. The activation energy along the diffusion path determines the percolation energy.

For calculations of $Mg_{0.3}Mn_2O_4$ percolation energy, a cubic spinel structure was assumed, using an occupancy factor of 0.3 in tetrahedral 8a sites. The Mn-deficient and O-deficient phases were also calculated using the adequate occupancy factor in the corresponding crystallographic sites, 16d and 32e respectively.

Electron Microscopy

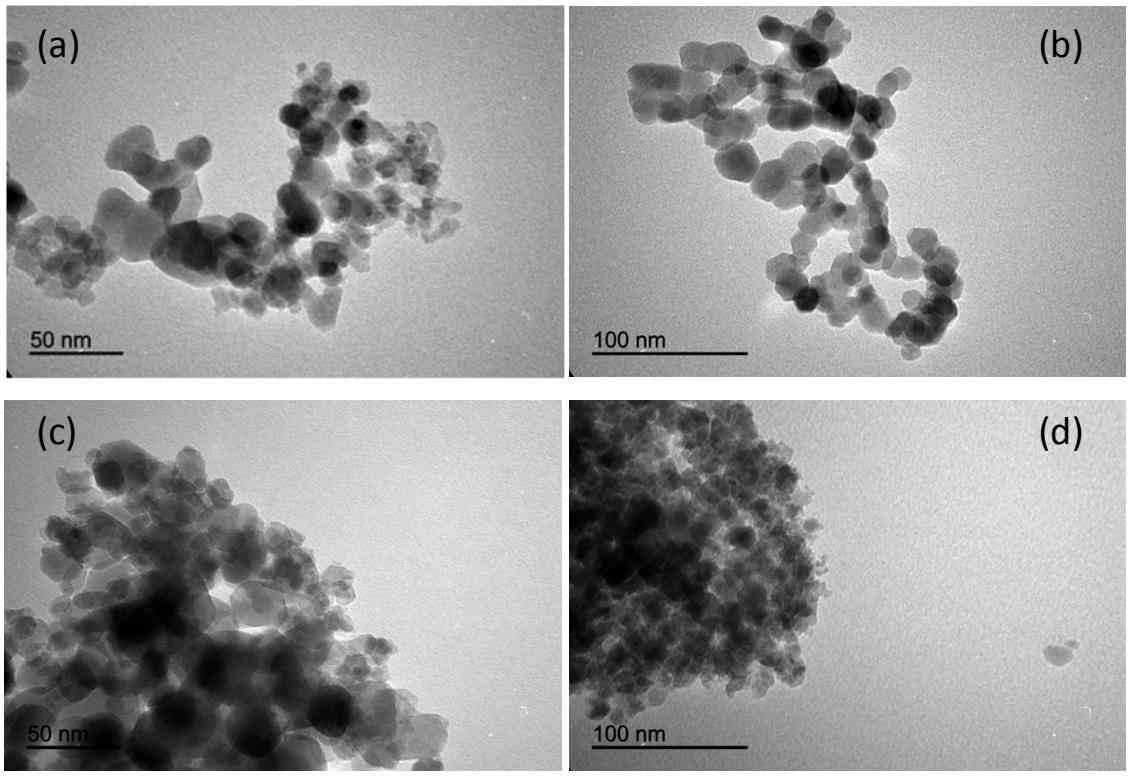

Figure S2. TEM micrographs of $MgMn_2O_4$ before (a, b) and after (c, d) acid treatment.

Impedance spectroscopy

The measurements of Electrochemical Impedance Spectroscopy (EIS) were performed in a VMP instrument, using the concentration cell previously described in this work. The amplitude of the signal was 10 mV.

The results of EIS (Fig. S3) show that the size of the depressed semicircle is smaller for the negative electrode compared to the positive electrode. This result agrees well with an easier magnesium (des)intercalation in the acid-treated sample, very probable due to the cationic vacancies.

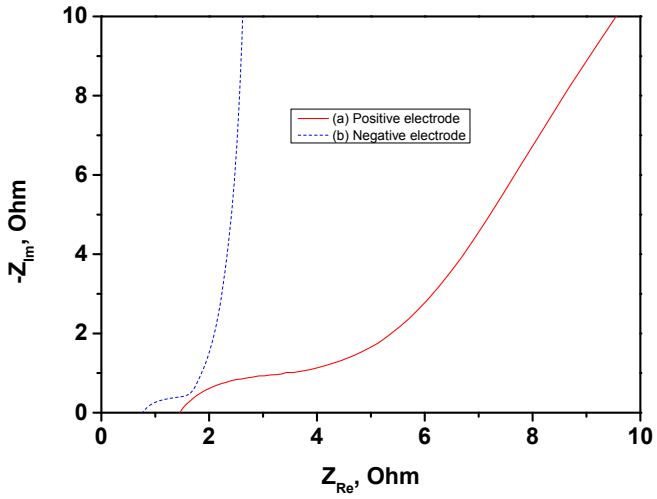

Figure S3. Impedance spectra obtained in the third cycle of a concentration cell. (a) EIS for the positive electrode at 2.4 V vs. Mg. (b) EIS for the negative electrode at 1.1 V vs. Mg.